puters and Structures, 79(14), p.p.1335-1353.
5. Zhao Xiangyang, Lai Kangsheng, Dai Dongming (2007) An Improved BP Algorithm and Its Application in Classification of Surface Defects of Steel Plate. *Journal of Iron and Research*, 14(2), p.p.52-55.
6. Ibnkahla, Mohamed (2002) Statistical Analysis of Neural Network Modelling and Identification of Nonlinear Systems with Memory. *IEEE Transactions on Signal Processing*, 50(6), p.p.1508-1518.
7. Youshen Xia, Leung, Henry, Wang Jun (2002) A Projection Neural Network and Its Application to Constrained Optimization Problems. *IEEE Transactions on Circuits &Systems Part I*, 49(4), p.p.447-459.
8. Setiono, Rudy, Wee KhengLeow, Zurada, Jacek M. (2002) Extraction of Rules from Artificial Neural Networks for Nonlinear Regression. *IEEE Transactions on Neural Networks*, 13(3), p.p.564-578.
9. Ishida H, Kaneko S, Tsujita W.et a1.(2009) Improvement of measurement accuracy in environmental monitoring system based on semiconductor gas sensor. *Transactions of the Institute of Electrical Engineers of Japan*, 125(6), p.p.245-252.
10. Frank D, Birgit K, Gunter G.(2003) Genetic algorithms and neural networks for the quantitative analysis of ternary mixtures using surface plasmon resonance. *Chemometrics and Intelligent Laboratory Systems*, 65(1),p.p.67-8l

Intelligent Solar Power Management Based on Fuzzy Logic Control

Lei Feng, Chunhui Liang

School of Electrical and Information Engineering,
Changchun Institute of Technology, Changchun, 130012,
China

Suli Zhang

School of Computer Technology and Engineering,
Changchun Institute of Technology, Changchun, 130012,
China

Abstract
This paper presents the intelligent charging and discharging management method for the solar power management circuitry based on fuzzy logic control theory. The mathematical model of DCDC circuit is established, and through Matlab theoretical derivation the feasibility of the maximum power point tracking by the method of obtaining the maximum output current through control is proven. And the experimental results confirm the theoretical rationality and correctness of the tracking of the maximum power point through the method of by sampling the maximum output current, to achieve the optimal solar charging

and discharging control of the power management circuitry, with low circuit cost and high stability and reliability.
Key words: MAXIMUM POWER POINT TRACKING (MPPT), FUZZY LOGIC, DCDC, SOLAR ENERGY, POWER MANAGEMENT.

1. Introduction

In recent years, with the continuous development of wireless sensor network technology, and its expanding range of applications, more and more applications at home and abroad adopt the wireless sensor network technology [1]. Meanwhile, with the development of the research on the Internet of Things in recent years, the function of the nodes of the Internet of Things that makes use of the wireless sensor network technology is constantly increasing. In addition to the data acquisition function, control function, LAN networking function, wide area networking function and other new functions are gradually integrated into the wireless sensor node [2]. Typically, accompanied with the increase of the node functionality, the working time of the node is also increasing, so is the power consumption of the node accordingly. But for outdoor work the adoption of solar power and charging, and the wireless sensor node with the battery energy storage mode, the energy supply of the node is limited. In the case of only limited energy supply at the node, the power supply circuit of the node will undoubtedly determine whether the node can be running in a long-term stable and reliable manner. The power management circuitry with good performance will make full use of the ambient energy, and convert it to the battery energy storage and rationally use the energy stored in the sensor nodes so as to extend the battery life to the maximum. [3].

People power the wireless sensor network node through the conversion of the solar, wind, vibration, and electromagnetic energy and other natural energy into electricity [4]. In the existing research results, Prometheus [5], AmbiMax [6] and other systems are power supply systems designed for the wireless sensor network. However, compared with other energy sources, as solar energy is easily accessible, and environmentally friendly, with the continuous characteristics of power supply, the adoption of solar-powered wireless sensor node mode for wireless sensor node power supply circuit is widely used. And there are relatively more of the related solar power supply circuit systems. For example, Prometheus designed solar energy based photovoltaic panel charging super capacitor and two level storage of lithium battery for the power supply circuit, the first level applies the super capacitor for energy storage, and the second level applies lithium battery for energy storage [7]. The management circuit in the circuitry is mainly responsible to manage whether to charge or discharge the lithium batteries, but the management circuit is not able to perform MPPT to solar energy, thus not able to achieve full utilization of energy. With respect to the Prometheus system, AmbiMax designed by C.Park et al. adopts the maximum power point tracking method to store the solar panel output energy into the capacitor, and the system also collects wind energy to charge the super capacitor. However, due to the relatively larger capacitance of the selected super capacitor, the power leakage phenomenon of the super capacitor is also very serious, the greater the capacitance, the larger the leakage current will be, and at the same time, the higher the super capacitor voltage is, the larger the leakage current of the capacitor will be, and the system does not handle the power leakage problem of the super capacitor very well [8]. For the power leakage problem of the super capacitor, Twinstar system adopts the leak sensor feedback control technology and energy synchronous technology, and basically realizes the long and persistent power supply for the super capacitor power supply nodes [9]. Durta et al. designed the Trio system which was the solar-powered wireless sensor network gateway system, however, as the node is responsible for the network communication needs for energy, the system uses a large area of solar panel to power the system, and the solar panel power is larger, which has not achieved low energy consumption at the nodes [10]. And Heliomote system uses photovoltaic panel to directly charge AA rechargeable batteries, which will cause the decline in the power supply performance of the battery, and at the same time will also have relatively low energy usage efficiency, without achieving a reasonable power management, and wasting part of the solar energy [11].

In this paper, the research content is the solar energy charging and discharging power management circuitry for the wireless sensor network nodes. As the selected ambient energy harvesting module is solar panel, while its output voltage and current characteristics are not stable, which is greatly influenced by light, temperature and other factors, and the output characteristics of the solar cell panel also contains a maximum power point output characteristic, in order to ensure that under different light and temperature conditions, the maximum utilization of the output en-

ergy of the solar panel requires a power management circuitry to achieve the maximum energy collection of the output energy of the solar panel. Meanwhile, as the storage element is rechargeable battery, the power management circuitry also needs to ensure reasonable charging and discharging management on the rechargeable battery, so that the rechargeable battery is neither overcharged, nor over-discharged. In short, the function of the power management circuitry is to maximize the utilization of input energy and output energy of the node system, to realize the self-sufficiency of the energy of the node in the wireless sensor network, to maximize the battery life, maintain permanent operation of the wireless sensor node, and extend the working life of the node.

2. Power Management Circuitry Operational Principle

2.1 Mathematical Model of Solar Panel

Firstly, let's introduce the mathematical model of the silicon cell unit for the solar panel; the silicon cell unit for the solar panel has a single diode equivalent circuit, as shown in the following diagram.

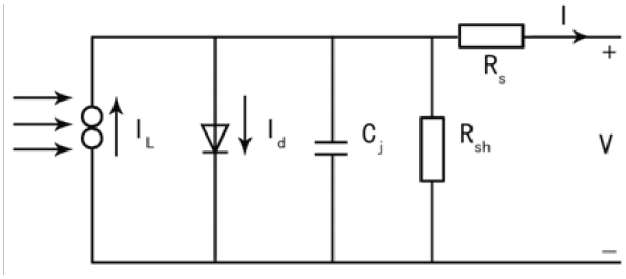

Figure 1. Solar Battery Single Diode Equivalent Circuit Diagram

In silicon cell single diode equivalent circuit, make the solar cell unit equivalent to a diode connected in parallel with a power supply, the electric resistance in the silicon diode material is equivalent to a series resistor R_s and a parallel resistor R_{sh}, while the PN junction capacitance is represented by C_j.

Under certain light intensity, the photocurrent I_L generated by silicon cell can be regarded as a constant current source generated by the silicon diode. Due to the very little impact of the junction capacitance C_j to I, it can be ignored in the theoretical analysis. Thus according to the current and voltage parameters, and then use Kirchhoff's Current Law, equation (1) can be obtained. The IV equation corresponding to the mathematical model of silicon cell for this equation is:

$$I = I_L - I_o\left\{\exp\left[\frac{q(V+IR_s)}{AKT_s}\right]-1\right\}-\frac{V+IR_s}{R_{sh}} \qquad (1)$$

Where:

I_o is the reverse saturation current of the silicon diode, with the unit A.

T_e is the absolute temperature of the silicon battery, with the unit K.

A is the diode factor.

q is the electron charge quantity $\left(1.6*10^{-19}℃\right)$.

K is Boltzmann's constant $\left(1.38*10^{-23}\ J/K\right)$.

In a typical analysis, R_{sh} is very large, and can be approximated to infinity, ignore $\frac{V+IR_s}{R_{sh}}$, equation (1) can be simplified to:

$$I = I_L - I_o\left\{\exp\left[\frac{q(V+IR_s)}{AKT_e}\right]-1\right\} \qquad (2)$$

Thus the silicon cell diodes single exponential mathematical model is obtained. In this paper, an improved and simplified nonlinear mathematical model commonly used in engineering based on equation (2) is adopted; the model utilizes the nominal parameters provided by the manufacturer, and ignores some secondary factors to constitute the aforementioned mathematical model. According to the nominal parameters of the silicon solar cell such as Isc, Voc, Im, Vm, Pm, etc., as provided by the manufacturer, the output voltage, output current, and output power of the silicon solar panel at certain temperature and light condition can be obtained through the mathematical model.

In consideration of the influence of the change of the solar radiation intensity and the temperature, the Reference documentation proposed a simplified nonlinear engineering mathematical model formula for solar cell, as shown in the following

$$I = I_{sc}\left(1-C_1\left(e^{\frac{V-VD}{C_1V_{se}}}-1\right)\right)+DI \qquad (3)$$

Where

$$C_1 = \left(1-I_{st}/I_{se}\right)e^{\frac{V_m}{C_1V_{st}}} \qquad (4)$$

$$C_2 = \left(V_m/V_{os}-1\right)/\ln\left(1-I_m/I_{sc}\right) \qquad (5)$$

$$DI = a\cdot S/S_{mf}\cdot DT+\left(S/S_{mf}-1\right)\cdot I_{sc} \qquad (6)$$

$$DV = -\beta\cdot DT - R_s\cdot DI \qquad (7)$$

$$DT = T_o - T_{mf} \qquad (8)$$

Isc: The short circuit current of the solar panel under the reference conditions.

Voc: The open circuit voltage of the solar panel under reference conditions.

Im, Vm: The solar panel maximum power point corresponding current and voltage under reference conditions.

S, Tc: S for the solar radiation intensity, with the

unit W/m2; Tc for the solar cell temperature °C.

S_{ref}, T_{ref}: S_{ref} is reference solar radiation intensity, and generally taken as $1kW/m^2$, T_{ref} is the reference temperature of the silicon solar panel, and generally taken as 25 °C.

α: The current temperature variation coefficient under reference lighting conditions, with the unit $A/℃$.

β: The voltage temperature variation coefficient under reference lighting conditions, with the unit $V/℃$.

Wherein the silicon cell (mono-crystalline or polycrystalline) measured value is:

$$\alpha:=0.0012Isc(A/℃), \beta = 0.005Voc(V/℃).$$

Rs: For the series electric resistance of silicon solar panel (Ohm), the value of Rs is determined by the relationship of Rs and Isc, Voc, Im, Vm in Reference documentation, as shown in the following

$$R_s = \frac{\frac{V_{sc}}{\ln(I_{sc}/I_o)}\ln\left(\frac{I_{sc}-I_m}{I_o}\right)-V_m}{I_m} \quad (9)$$

In equation (9), usually at standard temperature and light intensity, $I_o/I_{sc} \approx 10^{-8} \approx 10^{-10}$, which often takes $I_o = 10^{-9} I_{sc}$ in engineering.

Using the mathematical formula in equation (3) - (9), this paper adopts the Simulink toolbox in MATLAB software to build the simulation module in Figure 2 for simulating the volt battery plate output characteristics.

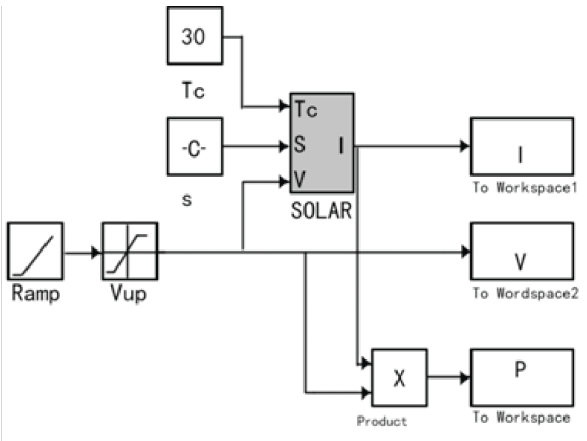

Figure 2. Solar Panel Output Characteristic Simulink Simulation System

2.2 Maximum Output Current Based MPPT Principle

In this paper, the solar charge control circuit performs the MPPT through tracking DCDC converter circuit maximum output current mode. In the control algorithm, the fuzzy logic control algorithm is applied, and the basic principle diagram of DCDC current is shown in Figure 3.

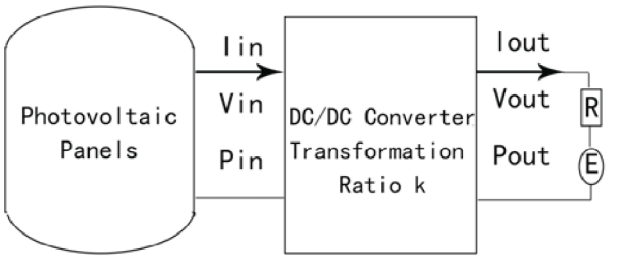

Figure 3. Solar Photovoltaic Panels and Linear Load by DCDC Converter Connection Diagram

In figure 3, the photovoltaic panels through DCDC converter network connect with linear load, since the main load herein includes battery and capacitor, both loads can be represented by the linear load model of a direct-current resistance and a voltage source in series.

2.3 DCDC Converter Circuit Design

In this paper, the DCDC circuit load is sealed valve regulated lead acid battery, where the battery is equivalent to a voltage source E in series with an electric resistance R, then

$$V_{oet} = E + I_{out} \times R \quad (10)$$

The following analysis is the influence of Iout on Pin.

In the equation (3), both sides is multiplied by Iout, and then combined with equation (1), it can be further derived that:

$$P_{in} = \frac{R \cdot I_{out}^2 + E \cdot I_{out}}{\eta} \quad (11)$$

As can be seen from equation (11), the output power Pin of the solar panel has a positive correlation property with the converter output current Iout, which means that Iout has the maximum value, and the corresponding Pin also has a maximum value. In other words, the maximum output current of DCDC circuit is the solar panel's maximum power point tracking.

Next is the analysis on the influence of K on Iout.

When the photovoltaic cell panel output voltage is Vin, then the corresponding output current is Iin, substituted into the equation (3) to get:

$$I_{in} = I_{DC}\left(1 - C_1\left(e^{\frac{V_{in}-DV}{C_1 V_{DC}}} - 1\right)\right) + DI \quad (12)$$

$$I_{in} = \frac{I_{out}}{\eta \cdot k} \quad (13)$$

From equation (10) it can be obtained that:

$$V_{in} = k \cdot E + k \cdot I_{out} \cdot R \quad (14)$$

Substitute equation (13) and (14) into equation

(12) to obtain

$$I_{out} = \eta \cdot k \cdot I_{DC}\left(1 - C_1\left(e^{\frac{k \cdot E + k \cdot I_{out} \cdot R - DW}{C_2 V_{DC}}} - 1\right)\right) + DI \quad (15)$$

Equation (15) is the transcendental equation on Iout and k. Let the accumulator battery load characteristic parameter E=4,R=0.1. The curve of equation (15) is drawn through Matlab tool.

When the value k starts to increase from 0, the curve value of Pin and Iout first increases and then decreases; when the k value reaches km, the inverter has the maximum output current value, while at the same time the photovoltaic cell has the maximum power output of Pm.

However, as E corresponds to the terminal voltage of the battery or capacitor, they are fixed within a certain period of time, and the corresponding R values at different voltages are also different. When the temperature or the light conditions change, the solar cell will have different values of Pm, in order to have real-time tracking of the solar cell's maximum power point, it is necessary to have real-time control on the corresponding k value of DCDC converter.

3. Fuzzy Logic Control Based Power Management

3.1 DCDC Converter Circuit Design

This paper selects the DCDC converter circuit of Sepic circuit for the maximum power point tracking and charging control. This paper selects the switching frequency of 50KHZ, if the switching frequency is selected too high, it will lead to an increase in the circuit switching loss, while if the switching frequency is selected too low, it will increase the output ripple voltage, therefore, the switching frequency selection is usually in range between 10K:-500K. But the switching frequency shall not be too small, such as the range of 10K-20K. Because for the sound with the vibration frequency of 20HZ-20KHZ, the human ear will pick up, and the frequency range that is especially sensitive to human ears is 2K-16KHz. Therefore, the switching frequency should not be selected too small. The selection of a switching frequency that is too small requires a relatively larger coupling capacitance Cs, this paper chooses 50KHZ mainly because the coupling capacitance Cs in the circuit in practice has the maximum of lOuF, and the affinity capacitance Cs value calculated by the adoption of the 50KHZ switching frequency happens to meet the requirements of less than lOuF, hence it is more appropriate to select the switching frequency as 50KHZ in this paper.

The topology design structure of Sepic circuit is shown as the following diagram:

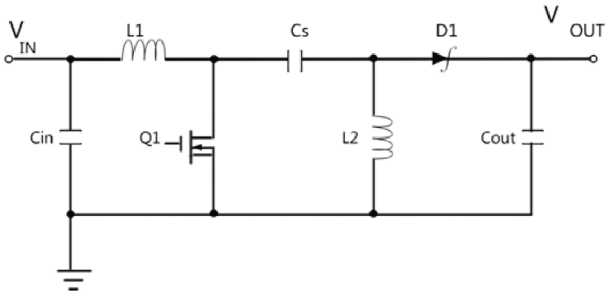

Figure 4. Topology Structure of Sepic Circuit

The MOS tube model selected by this paper: AOD472, MOSFET conduction resistance: $10m\Omega$.

Select passive components

1). The Calculation of Duty Ration

The calculation formula of the duty ration is as follows

$$D = \frac{V_{out} + V_d}{V_{in} + V_{out} + V_d}$$

$$\frac{D}{1-D} = \frac{V_{out} + V_d}{V_{in}} = \frac{I_{in}}{I_{out}}$$

As can be seen that there is Dmax when Vin(min), and there is Dmin when Vin (max).

When output Vout = 5.0V:

$$D_{\max} = \frac{V_{out} + V_d}{V_{in(\min)} + V_{out} + V_d} = \frac{5V + 0.3V}{1V + 5V + 0.3V} = 84.13\%$$

$$D_{\min} = \frac{V_{out} + V_d}{V_{in(\max)} + V_{out} + V_d} = \frac{5V + 0.3V}{7V + 5V + 0.3V} = 43.1\%$$

When output Vout = 0.5V:

$$D_{\max} = \frac{V_{out} + V_d}{V_{in(\min)} + V_{out} + V_d} = \frac{5V + 0.3V}{1V + 5V + 0.3V} = 44.4\%$$

$$D_{\min} = \frac{V_{out} + V_d}{V_{in(\max)} + V_{out} + V_d} = \frac{5V + 0.3V}{7V + 5V + 0.3V} = 10.26\%$$

2). Inductance Design

To design PWM switching converter, first we need to calculate the input inductance L1's ripple current, if the ripple current is too large, it will increases the EMI, while if it is too small, it will cause the instability of the PWM system, the compromise is to choose 20% to 40% of the input current.

When output Vout = 5.0V:

$$\Delta I_L = I_{in} \times \frac{30\%}{\eta} = I_{out} \times \frac{V_{out}}{V_{in(\min)} \times \eta} \times 30\% = 600mA \times \frac{5V}{1V \times 0.75} \times 30 \quad = I_{in} \times 30 \quad = 4A \times 30 \quad = 1.2$$

$$L1 = L2 = L = \frac{Vin(\min)}{\Delta I_L \times f_{sw}} \times D_{\max} = \frac{1V}{1.2 \times 50k} \times 0.84 = 14uH$$

When output Vout = 0.5V:

$$\Delta I_L = I_{in} \times \frac{30\%}{\eta} = I_{out} \times \frac{V_{out}}{V_{in(\min)} \times \eta} \times 40\% = 600mA \times \frac{5V}{1V} \times 40 \quad = 120mA$$

$$L1 = L2 = L = \frac{Vin(\min)}{\Delta I_L \times f_{sw}} \times D_{\max} = \frac{1V}{120mA \times 50k} \times 0.44 = 74uH$$

The peak current of inductance L1 and L2 is:

$$I_{L1(peak)} = I_{in} \times \left(1 + \frac{30\%}{2}\right) = 4A \times 1.15 = 4.6A$$

$$I_{L2(peak)} = I_{out} \times \left(1 + \frac{30\%}{2}\right) = 600mA \times 1.15 = 0.69A$$

For L1 and L2 coupled inductance can be adopted, as the coupled inductance has two inductors wound on the same core, due to the inductive coupling, the inductance value of L1 and L2 should be replaced by 2L. In this case the corresponding coupled inductance value can be thus calculated:

$$L1' = L2' = \frac{L}{2} = 37uH$$

This paper selects 100uH and 150uH inductance, which leakage inductance values are both between 15uH ~ 20uH. And the turns ratio is preferably 1: 1, as for the given output voltage ripple, the coupled inductance value is half of the independent inductance value.

3.2 MPPT Control Algorithm Design

MPPT control algorithm, that is, the maximum power point tracking algorithm, is through sampling the DCDC converter output current, by adjusting the duty ration of the PWM output, to achieve accurate tracking of the maximum power point of the solar cell panels. It would be preferable to adopt efficient algorithm to achieve maximum power point tracking, the more streamlined the algorithm is, the faster the execution of the maximum power point tracking will be, and the smaller the corresponding power consumption will be.

Due to the great influence of the light, temperature and other environmental factors on the output characteristics of the solar panel, for solar energy charging control algorithm, this paper selects the better robustness, and better dynamic and static performance, the MPPT control algorithm in this paper selects the fuzzy logic control algorithm, which can adapt to the changes in the external environment very well, and also eliminate the residual error existed in the fuzzy logic control algorithm, and the control principle of the algorithm is that, when the input deviation is large, using the fuzzy logic algorithm with fast adjustment rate to control, to obtain a better dynamic adjustment feature. And when the deviation is small, adopt n-integral control to eliminate residual error existed in the system by integration, to get a better steady state performance. The algorithm is well adapted to the change of output characteristics of the solar panels under different conditions of light and temperature, to achieve the maximum power point tracking of the solar cell panel output characteristics.

The algorithm structure diagram is shown in Figure 5.

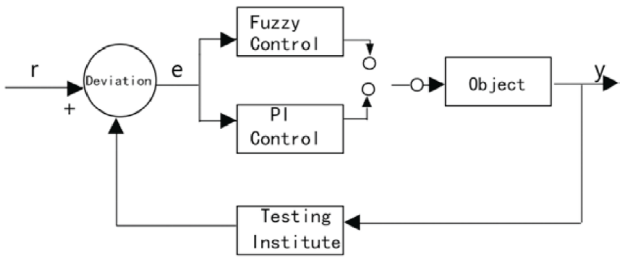

Figure 5. Fuzzy - PI Dual-mode Control System Structure Diagram

3.3 Realization of the fuzzy algorithm of the maximum power point tracking

According to the requirements herein, the control parameter in this paper is the output current of DCDC circuit, set the fuzzy language variable of the corresponding deviation as x, the fuzzy domain as [-50,50], the fuzzy language variable of the deviation change

rate as y, the fuzzy domain as [-100,100], the output language variable as dD, and the fuzzy domain as [-50,50]. The unit corresponding to the fuzzy domain is mA. Here we define 3 fuzzy variables, the deviation x, deviation change rate y, and the output control volume dD. They are all constituted by 8 fuzzy language values {NB, NM, NS, NO, PO, PS, PM, PB}, and corresponding to {negative large, negative medium, and negative small, negative zero, positive zero, positive small, medium, positive large} respectively. According to the aforementioned fuzzy variable definition, the fuzzy logic rule table corresponding to the maximum power point tracking algorithm adopted by this paper is shown in Table 1, where the yellow area is output volume dD.

Table 1. Maximum Power Point Tracking Fuzzy Control Rule Table

Maximum		X							
		NB	NM	NS	NO	PO	PS	PM	PB
y	NB	PB	PM	PS	PO	NO	NS	NS	NB
	NM	PB	PM	PS	PO	NO	NO	NS	NS
	NS	PM	PS	PS	PO	NO	NO	NO	NS
	NO	PS	PS	PO	PO	NO	NO	NO	NO
	PO	NO	NO	NO	NO	PO	PO	PS	PS
	PS	NS	NO	NO	NO	PO	PS	PS	PM
	PM	NS	NS	NO	NO	PO	PS	PM	PB
	PB	NB	NS	NS	NO	PO	PS	PM	PB

4. Power Management Experiment

In the MPPT testing, this paper connects the solar power management circuits to 4.5V, 3W solar panel input DCDC converter, to measure the photovoltaic cell output power Pin and the inverter output current Iout at different scale factor k, to obtain the curve from the experiment as shown in Figure 6 The experiment measures the ambient light intensity parameter is 45700Lux, temperature 5 °C. As can be seen from the curve in Figure 6, with the increase of the k value, photovoltaic cell output power and the inverter output current are first increased and then reduced, and both achieving the maximum at the same value of k = 0.8, and the experimental data shows that by detecting the output current of the inverter, and then by adjusting the value of k, then the solar panel maximum output power point (maximum power point) tracking can be realized, and the experiment data verifies the maximum power point tracking algorithm of the DCDC circuit based maximum output current in section 3.3.2.

The above diagram is a comparative experiment of the lead-acid battery charging current carried out at around 9 o'clock on July 31, 2015, when the ambient temperature was of the light intensity 28200LUX, temperature 25V. As can be seen from the curve in the figure 7, under the premise of the same environmental conditions, the charging current by adopting the MPPT tracking charging circuit in this paper can reach about 3 times of the charging current adopting CN3082 charging current, indicating that the use

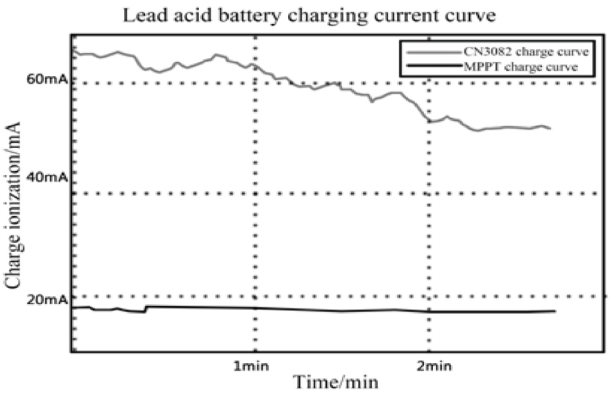

Figure 7. MPPT Charging and CN3082 (Non MPPT) Charging Comparative Test Data

of MPPT tracking charging method is more able to make full use of the energy output of solar panels to realize the fuller utilization of solar energy.

5. Conclusion

The main work of this paper realized the solar energy management circuit sampling principle through DCDC circuit output current, and made use of fuzzy logic algorithm to achieve maximum power point tracking, and store the maximum solar panel output energy in the accumulator. When the accumulator is fully charged, the solar panels directly supply the load circuitry through super capacitor, and DCDC circuit has constant voltage charging control to the super capacitor, so as to ensure the serving life of the lead-acid battery, and finally design the solar cell charging and discharging power management circuitry with MPPT, PM and DPPM, and successfully

applies to the relevant online measurement projects. In this paper, the solar cell charging and discharging power management circuit has a charging efficiency above 80%, and the power management circuit static operation current is less than 1mA, at different light intensities, to carry out dynamic power management intelligently, thus the stability and reliability of the circuit is extremely high.

Acknowledgments

This paper is a scientific and technological project of the "Twelfth Five Year Plan", with the project name *Wireless Sensor Network Based Agricultural Farmland Intelligent Platform Construction*, Project No.: 120120060.

References

1. Lalouni S., Rekioua D., Rekioua T. (2009) Fuzzy logic control of stand-alone photovoltaic system with battery storage. *Journal of Power Sources*, 193(2), p.p.899-907.
2. Jiang X., Polastre J., Culler D. (2013) Perpetual Environmentally Powered Sensor Networks. *Proc. of Fourth International Symposium on Information Processing in Sensor Networks*, p.p. 463-468.
3. Park C., Chou P.H. (2015) Ambi Max: Autonomous Energy Harvesting Platform for Multi-supply Wireless Sensor Nodes. *Proc. of the 3rd Annual IEEE Communications Society on IEEE*, p.p. 168-177.
4. Dutta R., Hui J., Jeong J., et al. (2012) Trior Enabling sustainable and sealable outdoor wireless sensor network deployments. *Proceedings of the 5th international conference on Information processing in sensor networks*, p.p. 407-415.
5. Lin K., Yu J., Hsu J. et al. (2011) Heliomote: Enabling Long-lived Sensor Networks Through Solar Energy Harvesting. *Proceeding of the 3rd international conference on Embedded Networked Sensor Systems*, p.p. 309.
6. Meninger S., Mur-Miranda O. J., Amirtharajah R. Chandrakasan, Lang A. J. (2013) Vibration-to-electric Energy Conversion. *IEEE Transaction on Very Large Scale Integration Systems*, 21(1), p.p.64-76.
7. Want R., Res I. (2014) An Introduction to RFID Technology. *IEEE Pervasive Computing*, 15(1), p.p.25-33.
8. Raghunathan V., Kansal A., Hsu J., et al. (2015) Design Considerations for Solar Energy Harvesting Wireless Embedded Systems. *Proceedings of Embedded Sensor Network Systems*, p.p. 24-27.
9. Park C. and Chou P. (2008) Power Utility Maximization for Multi-supply Systems by A Load-matching Switch. *International Symposium on Low Power Electronics and Design*, p.p. 56-65.
10. Brunelli D., Moser C., Thiele L. (2009) Design of A Solar-harvesting Circuit for Battery less Embedded Systems. *IEEE Transactions on Circuits and Systems I*, 56(11), p.p.2519-2528.
11. Corke P., Valeneia P., Sikka P., et al. (2010) Long-Duration Powered Wireless Sensor Networks. *Proceedings of the 4th workshop on Embedded networked sensors*, p.p. 33-37.